DISCUSSION AND CONCLUSION

A typical pressure distribution predicted by the above equation is plotted in arbitrary units (Figure 2). In the vicinity of the aeration section, the change of pressure with θ is considerable. Moving up from the aeration section, however, the change with θ becomes smaller, as the aerating gas is more evenly distributed across the hopper. There are no experimental data available showing the variation of fluid pressure with both θ and r. However the experimental measurements by the author, of the fluid pressure along the centerline of a discharging plane hopper for various air inputs were compared with the corresponding equations for the two dimensional case.

The test hopper consisted of two inclined walls held together by two parallel plexiglass plates. It was arranged so that the hopper angle and the orifice width could be varied. Aeration was achieved by blowing air through two porous sections on the inclined walls extending from r_0 to r_2 (Figure 1). The results were obtained with sand of 276 μm surface-volume mean diameter and 2,640 kg/m^3 solid density. Permeability constant given by Carman-Kozeny expression, $K_p = d^2\phi^2\epsilon^2/180(1-\epsilon)^2\mu$ was used in the calculations (Carman 1937). Bed voidage of 0.522 was obtained by curve fitting one set of results, and was used for all the other air flow rates. Sphericity of sand was taken as 0.8.

In Figure 3, experimental results for three different aeration rates are shown in arbitrary units, together with the calculated pressure from the above theory. Agreement between the theoretical predictions and the experimental results is very good, and so supports the basic approach to the present theory. The close agreement with theory along the whole height of the hopper also verifies the assumption of constant hopper voidage. It is hoped that this analysis of the fluid pressure distribution will serve as a useful tool in the analytical study of aerated hoppers, whether the concern is the stress analysis, solids discharge rate, or any other aspect where fluid pressure has an influence.

ACKNOWLEDGMENT

Valuable discussions with Professor J. F. Davidson are gratefully acknowledged.

NOTATION

d = mean particle diameter
K_p = permeability constant
p = fluid pressure
r = radial coordinate
r_0, r_1 = radial positions of orifice and top surface respectively
r_2 = radial position of the end of aeration section
s = $\ln(r/r_0)$
u = interstitial fluid velocity
U_a = gas flowrate per unit area of aeration section
v = particle velocity
x = r/r_0

Greek Letters

α = half included hopper angle
ϵ = bed voidage
ϕ = sphericity of particles
θ = angular coordinate
λ = constant defined by Equation (8)
μ = fluid viscosity
ω = $\cos\theta$
Λ = $\lambda(\lambda+1)$

LITERATURE CITED

Altiner, H. K., "Flow of partly fluidised particles," Ph.D. thesis, University of Cambridge (1975).

Bird, R. B., W. E. Stewart, and E. N. Lightfoot, *Transport Phenomena*, Wiley & Sons, New York (1960).

Carman, P. C., "Fluid flow through granular beds," *Trans. Inst. Chem. Eng.*, **15**, 150 (1937).

Davidson, J. F., and D. Harrison, *Fluidized Particles*, Cambridge Univ. Press, Ch. 4 (1963).

Dixon, W. G., Private communication, University of Cambridge (1974).

Papazoglou, C. S., and D. L. Pyle, "Air-assisted flow from a bed of particles," *Powder Tech.*, 4(1), 9 (1970).

Manuscript received June 13, and accepted July 10, 1979.

Effect of an Array of Objects on Mass Transfer Rates to the Tube Wall: An Additional Note

ALEKSANDAR P. DUDUKOVIĆ

Institute for Petrochemistry, Natural Gas, Oil and Chemical Engineering, Department of Chemical Engineering, Faculty of Technology, Novi Sad, Yugoslavia

and

SLOBODAN K. KONCAR-DJURDJEVIC

Department of Chemical and Metallurgical Engineering, Faculty of Technology and Metallurgy, Beograd, Yugoslavia

In previous publications (Končar-Djurdjević and Duduković 1977, Duduković and Končar-Djurdjević 1979) we described the effect of a single object and of an array of disks on mass transfer rates to the wall of a coaxial cylindrical tube. In this note we intend to give a short review of experimental results obtained in the case of an array of spheres, as well as to indicate the differences of the effects of an array of disks and the array of spheres on mass transfer rates to the inside wall of a coaxial cylinder (Figure 1).

The apparatus used, measurement method, and all working conditions are the same as described (Duduković and Končar-Djurdjević 1979).

The experiments were carried out for a pair of spheres, each 47.6mm in diameter, i.e. for the ratio of sphere to tube diameter $d_p/d = 0.793$ and at the Reynolds number of $Re = 47{,}600$, for

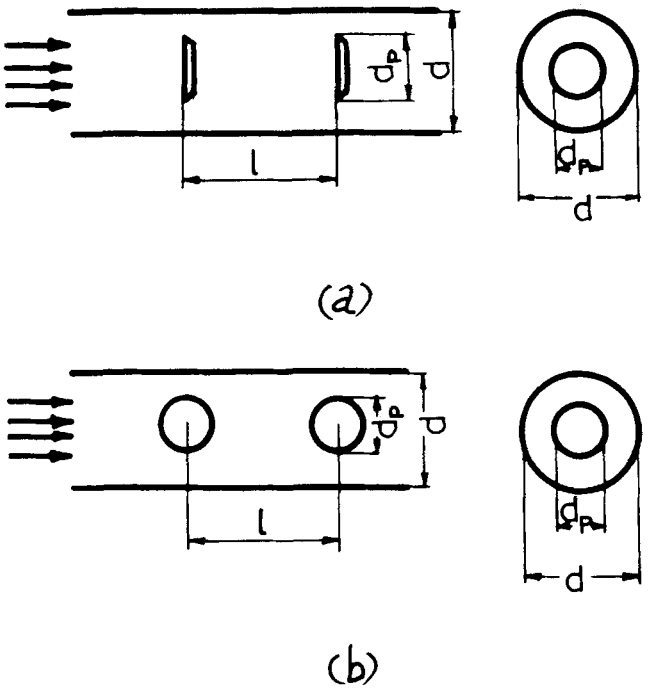

Figure 1. Position of objects in tube: a) disks, b) spheres.

various dimensionless distances between the spheres l/d_p. In Figure 2 and Figure 3, typical results for $l/d_p = 1.00$ and $l/d_p = 2.15$, are given respectively. Results are shown as the dependence of a local dimensionless Sherwood number Sh/Sh_∞ on the distance along the tube x, where Sh is the local Sherwood number, and Sh_∞ the local Sherwood number sufficiently far from the sphere, i.e., the Sherwood number which characterizes an undisturbed stream in the tube. The positive direction of the x-axis is in the direction of fluid flow, and $x = 0$ is a normal projection of the center of the first sphere on the tube wall.

The curves in Figures 2 and 3 retained some characteristics of those for individual objects, as well as for the array of disks. All of these curves have local extremes near the object. But comparing Figures 2 and 3 with the corresponding results for the array of disks (Dudukovic and Končar-Djurdjević 1979) indicates that besides some common characteristics, there are some essential differences.

The appearance of two local minima on the curves $Sh/Sh_\infty = f(x)$ indicates that after each sphere, a separate wake is formed. Such a local minimum behind each sphere is the result of fluid suction into the wake, which increases the thickness of the boundary layer at the tube wall. Immediately after each local minimum, there is a sudden rise of the local Sherwood number and a local maximum. This maximum results from the instability of the wake and its separation. These lead to a deep penetration of highly turbulent pulsations into the laminar sublayer, thus decreasing the thickness of the diffusion sublayer. More detailed analyses of all of the local extremes on the curves $Sh/Sh_\infty = f(x)$ were already given (Končar-Djurdjević and Dudukovic 1977, Dudukovic and Končar-Djurdjević 1979).

For the pair of disks, it was characteristic that at the distances smaller than $l/d_p \approx 1.7$, there was no stable wake behind the second disk. Its formation was disturbed by the existence of the wake behind the first disk. Thus, two disks at small distances behaved essentially as one object, and only one minimum and maximum was observed on the $Sh/Sh_\infty = f(x)$ curve. On the contrary, in the case of spheres even at the smallest possible distance ($l/d_p = 1.00$), this is not the case.

At the smallest distance (Figure 2), the second sphere affects the length and the shape of the wake behind the first one. The second local maximum of the first sphere overlaps with the first local maximum of the second one. At greater distances this is not

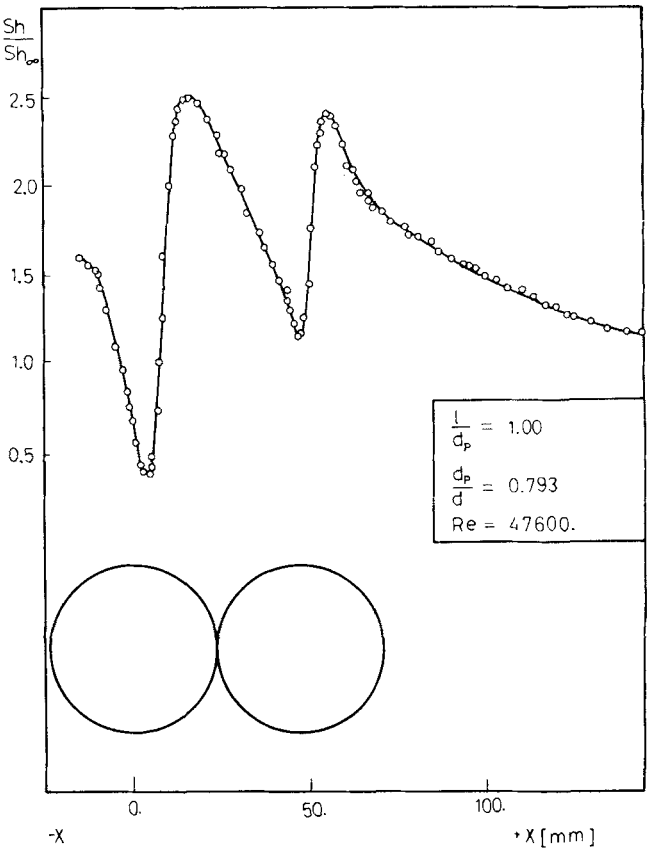

Figure 2. Local Sherwood number as function of distance ($l/d_p = 1.00$, $Re = 47600$).

so. As well as with the pair of disks, at greater distances (e.g., $l/d_p = 2.15$, Figure 3), the curve $Sh/Sh_\infty = f(x)$ has the characteristic shape with two local maxima and one local minimum in the area of each sphere, which is typical behavior for a single object. The

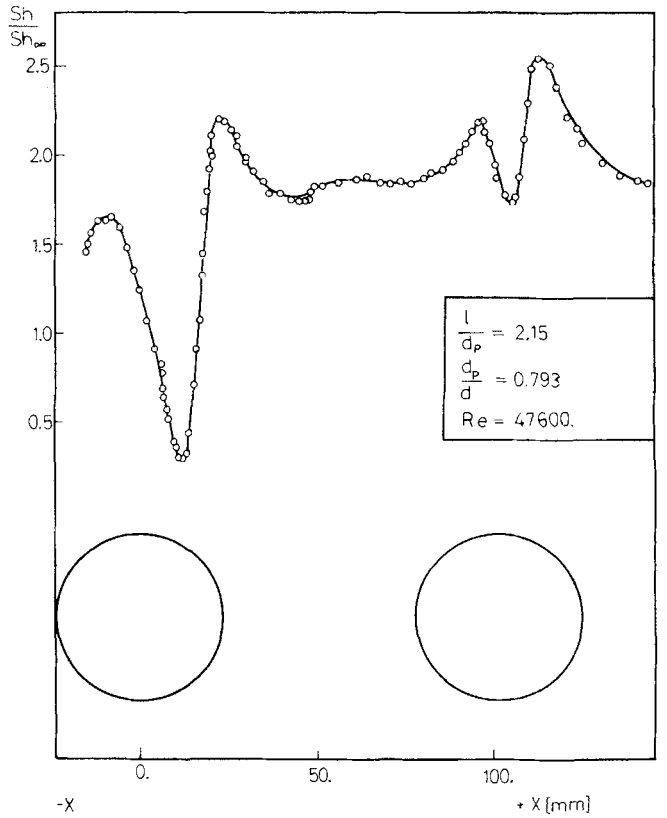

Figure 3. Local Sherwood number as a function of distance ($l/d_p = 2.15$, $Re = 47600$).

values of the local Sherwood numbers for the second sphere are greater, due to the greater intensity of turbulent pulsations, caused by the presence and instability of the first wake.

These results indicate that, although mass transfer enhancement to the tube walls can be achieved by positioning an array of objects into the tube, the magnitude and distribution of local Sherwood numbers depends not only on Re, l/d, d/d_p (as found in previous work), but also on the type of objects used. The maximum and average Sherwood numbers are much higher in the case of two disks than for two spheres. Positioning of disks seems to be more favorable, not only because it yields higher mass transfer coefficients, but also because the pressure drop at an l/d_p ratio of 0.6 is smaller than the pressure drop in case of a single disk. Such effect cannot be achieved with spheres.

NOTATION

d = tube diameter
d_p = sphere diameter
l = distance between the spheres
Sh = local Sherwood number
Sh_∞ = local Sherwood number characteristic for undisturbed stream in the tube
x = distance along the tube

LITERATURE CITED

Duduković, A. P., and S. K. Končar-Djurdjević, "The Effect of an Array of Disks on Mass Transfer Rates to the Tube Wall," *AIChE J.*, **25**, 895 (1979).

Končar-Djurdjević, S. K., and A. P. Duduković, "The Effect of Single Stationary Objects Placed in the Fluid Stream on Mass Transfer Rates to the Tube Walls," *AIChE J.*, **23**, 125 (1977).

Manuscript received November 13, 1978; revision received July 26, and accepted August 29, 1979.

Rectilinearity Rule for Vapor and Liquid Densities Along the Azeotropic Locus

AMYN S. TEJA

Department of Chemical Engineering
University of Delaware
Newark, Delaware 19711

The phase behavior of mixtures at high pressures is of great practical as well as theoretical interest. Of particular note is the behavior of mixtures which deviate from ideality, to an extent that azeotropes are formed. Extensive work by Kay and coworkers (Kay and Brice 1953a, Kay and Rambosek 1953b, Skaates and Kay 1964) has shown that mixtures that form azeotropes in the critical region exhibit a minimum or maximum temperature point in their critical locus curves (Figure 1). On a P-T projection, the azeotropic locus becomes tangential to the critical locus curve at the critical azeotropic point. Because of this behavior, the co-ordinates of the critical azeotropic point are difficult to establish both theoretically (Teja and Kropholler 1974) and experimentally.

Azeotropic mixtures, however, exhibit certain characteristics which are typical of pure substances. For example, Licht and Denzler (1948) have shown that the logarithm of the azeotropic pressure is an approximately linear function of the reciprocal temperature. More recently, Li (1977) has shown that a given azeotropic mixture follows a rectilinear equation of the type:

$$\left(\frac{\rho^V_{az} + \rho^L_{az}}{2\rho^c_{az}}\right) = 1 + A\left(\frac{T_{az} - T^c_{az}}{T^c_{az}}\right) \qquad (1)$$

where ρ^V_{az}, ρ^L_{az}, and ρ^c_{az} are the saturation densities of the vapor phase, the liquid phase, and of the critical azeotrope, respectively. T_{az} is the azeotropic temperature, T^c_{az} is the critical azeotropic temperature and A is a constant. Li, however, went on to suggest that A for the azeotropes could be calculated from the slopes A_i of the rectilinear equations for the pure components as follows:

$$A = \Sigma\, x_i A_i \qquad (2)$$

where x_i is the "mole fraction of component i." It is not obvious which mole fraction is to be used, since this quantity varies along the azeotropic locus in Figure 1.

Equation (1) is a form of the so-called "Law of Rectilinear Diameters" proposed by Cailletet and Mathias (1886) to describe the behavior of the densities of the coexisting phases of a pure fluid, as a function of temperature near the gas-liquid critical point. Analogous rules for pure fluids have been proposed for the slopes of isochores issuing from the coexistence curve (Hall and Eubank 1976); the thermal conductivities of the coexisting phases of ammonia (Needham and Ziebland 1965), and the viscosities of coexisting phases of the low molecular weight n-alkanes (Starling et al. 1962).

An extension of the rectilinear diameter equation to the densities of coexisting phases of binary mixtures at constant temperature was proposed by Won and Prausnitz (1974) and is of the form:

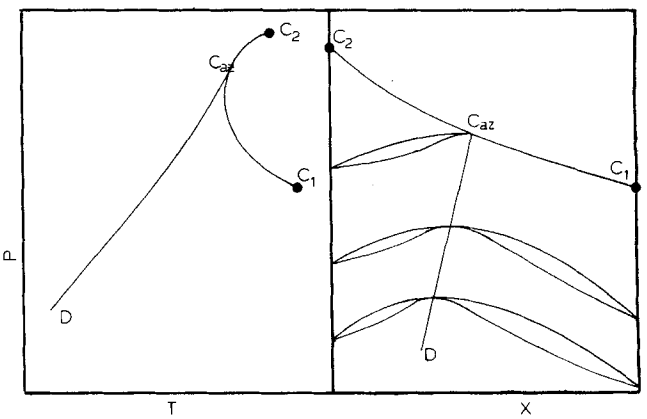

Figure 1. Schematic *P-T* and *P-x* diagrams for systems in which azeotropic behavior persists in the critical region. C_1, C_2 are the critical points of the pure components and C_{az} is the critical azeotropic point. The curve $C_1C_{az}C_2$ is the critical locus and the curve DC_{az} is the azeotropic locus.

Amyn Teja is on leave from the Department of Chemical Engineering, University of Technology, Loughborough, LE11, 3TU, England.